Hindawi
Geofluids
Volume 2018, Article ID 8947839, 10 pages
https://doi.org/10.1155/2018/8947839

WILEY | Hindawi

Research Article

Numerical Simulation of Residual Oil Flooded by Polymer Solution in Microchannels

Yang Liu, Jiawei Fan, Lili Liu, and Shuren Yang

Key Laboratory of Enhanced Oil and Gas Recovery, Ministry of Education, Northeast Petroleum University, Daqing 163318, China

Correspondence should be addressed to Jiawei Fan; fanjiawei@nepu.edu.cn

Received 20 October 2017; Revised 11 December 2017; Accepted 26 December 2017; Published 8 July 2018

Academic Editor: Zhenhua Rui

This paper establishes a flow equation using non-Newtonian fluid mechanics and defines the deformation of residual oil using numerical computation in order to conduct a study on the flow law of residual oil in microchannels of rock during polymer flooding, the influence of flooding fluid elasticity on the deformation of residual oil, and flooding mechanism of viscoelastic displacing fluid. Computation shows that advancing contact angle increases and receding contact angle decreases as the viscosity ratio decreases. The higher elasticity of polymer solution with higher concentration or molecular weight leads to significantly more obvious deformation of residual oil and benefits migration and stripping of residual oil. The impact of the initial wetting angle of residual oil film on deformation is analyzed. A smaller initial wetting angle corresponds to a bigger change of advancing contact angle and smaller change of receding contact angle. A better understanding of the flooding process is gained via a study on residual oil deformation in polymer flooding. Consequently, oil flooding efficiency and oil recovery can be enhanced. This is the hydrodynamic mechanism of enhanced oil recovery (EOR) by polymer flooding.

1. Introduction

There are two reasons why polymer solution greatly increases oil recovery of the oilfield flooded by water: (1) with higher viscosity, polymer solution effectively improves the oil-water mobility ratio, reduces the interlayer contradictions, improves the fluid entry profile, and increases the sweeping volume of flooding solution; (2) with viscoelastic effect, polymer solution floods the residual oil after water flooding and increases flooding efficiency and thus oil recovery. Zhang and Yue [1] studied the flooding mechanism of residual oil in the dead end and found that bigger viscoelasticity and sweeping volume of polymer solution led to stronger stress on residual oil. Jamaloei and Kharrat [2] conducted a detailed analysis of the mechanism of surfactant flooding in oil-wet and water-wet porous medium. Shi et al. [3] conducted a study on residual oil distribution by steam flooding after polymer flooding with a refined numerical method, which provides a reliable basis for further development of specified oilfield blocks. Seppecher [4] computed the flow of the fluid around contact line with numerical computation and figured out the relation between the dynamic contact angle and the static contact angle and its impact on velocity. Chou et al. [5] computed the change of advancing contact angle and receding contact angle of fluid drop on a tilting plane and wetting hysteresis with numerical computation, which was consistent with the experiment. Harvie et al. [6] conducted a parameter study on fluid drop deformation through fluid flow microshrinkage. Garstecki et al. [7] described the deformation process of fluid drops and gas bubbles in a microscale T-shape flow channel and pointed out that fluid drop bursting mainly depended on differential pressure in case of small capillary number. Fang et al. [8] conducted three-dimensional numerical simulation of contact angle hysteresis of microscale two-phase flow and discussed the deformation and separation conditions of fluid drops. Seevaratnam et al. [9] studied the water-driven deformation of fluid drops adhering to a solid wall under constant differential pressure and suggested that the deformation was influenced by the quantity of flow, viscosity ratio, and fluid drop volume. The critical condition of fluid drop sliding and separation was taken by a high-precision camera. Cubaud et al. [10] computed the coupling of fluid drop and viscous laminated flow in the square micro pore-throat and pointed

out that capillary number was an influencing factor for fluid drop bursting and analyzed the influence of fluid drop bursting to small fluid drops on the flow. Wang et al. [11–13] conducted in-depth research on how viscoelastic fluid improves flooding efficiency and pointed out that the elasticity of viscoelastic fluid changes the force on residual oil and thus improves the flooding efficiency. They defined microforces for the first time and illustrates that microforces accelerate the deformation and convex of residual oil and small oil drops are separated from the main body. Yang et al. [14, 15] figured out the flow equation of viscoelastic fluid in micro porethroats and numerical solution of flow field, including velocity field and stress field, with upper-convected Maxwell constitutive equation, compared the flooding force on residual oil by different viscoelastic flooding fluids and corresponding residual oil deformation, and obtained hydrodynamic mechanism of elastic flooding of residual oil drop. Rother et al. [16] studied the impact of the surfactant on the viscous interaction in buoyancy flooding of deformed drops. Xiao et al. [17–19] studied the influence of emulsion inertia on shearing, calculated the stress with the Batchelor formula to obtain the interfacial stress and disturbance stress, initially forming the dynamics mechanism of drops in oscillatory and elongational flow with limited Reynolds number and reflecting elastic effect of stress of viscous drop emulsion under inertia. Fu et al. [20] observed the deformation and bursting of fluid drop in transition from a drop shape to a jet shape in micro porethroats by experiment. Qi and Xu [21] obtained precise speed field and stress field through discrete Laplace transform of a series of fractional derivative, providing a good method for studying the fluid with complex rheological property. Zhang et al. [22] numerically studied the flow of fully developed viscoelastic fluid through a rotary quadrature tube and calculated axial velocity and axial normal stress. Calculation results show that secondary flow, axial flow, and axial normal stress are all influenced by rotation. Hayat et al. [23] calculated the rotational flow of generalized Newtonian fluid in porous media with the slip condition of wall taken into consideration and compared boundary conditions with slip and nonslip.

2. Mathematical Model

Residual oil refers to the crude oil remaining in the pores within the flooding area in the flooding process and is usually dispersed. Residual oil after water flooding can be classified into five types, that is, oil drop, oil column, oil film, oil cluster, and oil in a dead end, and oil film type has the largest quantity and the broadest distribution. The formation of residual oil is mainly influenced by the microscopic anisotropy of oil formation, wettability on the rock surface, and the interfacial tension between crude oil and water [24]. This paper treats oil film type residual oil as the study object and establishes a physical model of residual oil film on the surface of pores of a certain rock (Figure 1). It mainly studies the velocity and stress distribution of the flow field where polymer solution flood residual oil film, analyzes the impact of the viscosity ratio of flooding solution and residual oil and the wettability of residual oil on the stress and deformation

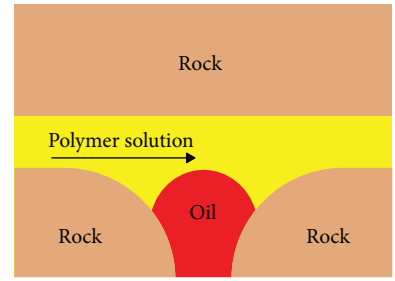

Figure 1: Physical model.

of residual oil, and finally figures out the hydrodynamics mechanism of polymer flooding.

2.1. Weissenberg Number. There are many rheological parameters to characterize fluid viscoelasticity in the study on the rheological property of viscoelastic fluid. This paper mainly adopts the Weissenberg number (We) to identify the ratio of elasticity to viscosity of fluid.

Different from pure viscous fluid, in addition to nonreversible deformation (viscous flow) under the external force, viscoelastic fluid flowing in the channel has a certain strain recovery and shows elasticity after the external force is gone. In order to represent the role of the elastic effect in flowing, a nondimensional number We is defined and it equates to recovery strain (elastic strain).

$$\mathrm{We} = \frac{N_1}{\tau}, \tag{1}$$

where We is defined as the ratio of the first normal-stress difference N_1 to viscous shear stress τ. When We is big, flowing is mainly determined by the first normal-stress difference: elasticity plays a leading role. When We is small, flowing is mainly determined by viscosity force. Therefore, the role elasticity and viscosity plays in the flowing of viscoelastic fluid can be clarified.

In the low shear laminated flow, we have

$$\mathrm{We} = \frac{J_e \eta U}{D}, \tag{2}$$

where J_e represents steady shear compliance with $J_e = 1/G$, G represents elasticity modulus, U represents characteristic velocity, and D represents characteristic scale.

Therefore, for viscoelastic fluid flowing in the channel, the characteristic scale can be set as the channel width, characteristic velocity can be set as the average velocity in the channel, and relaxation time is

$$\lambda = J_e \eta = \frac{\eta}{G}. \tag{3}$$

Then We can be calculated by the following formula:

$$\mathrm{We} = \frac{\lambda U}{D}. \tag{4}$$

Weissenberg number represents the elasticity of viscoelastic fluid. Elasticity plays a significant role in flooding, especially in the third recovery. On the one hand, the bigger

elasticity of viscoelastic fluid leads to a bigger sweeping area and higher sweep efficiency. On the other hand, the bigger elasticity of viscoelastic fluid leads to bigger normal stress and tangential stress on residual oil and makes residual oil deform more easily, increasing flooding efficiency. Given that recovery efficiency equals to sweep efficiency multiplied by flooding efficiency, increasing the elasticity (We) of viscoelastic fluid can enhance oil recovery. Viscoelastic fluid has a bigger influence on flooding efficiency.

The capillary number $\mathrm{Ca} = \mu_p Gh/\sigma$ represents the ratio of viscosity force to interfacial tension [25], μ_p represents the viscosity of polymer solution, μ_o represents the viscosity of residual oil, and the viscosity ratio of residual oil and the polymer solution is $\lambda_\mu = \mu_o/\mu_p$.

2.2. Motion Equation. Since the interface is moving, interfacial tension is taken into consideration in the motion equation [26, 27].

$$\frac{\partial(\rho u)}{\partial t} + \nabla\cdot(\rho uu) = \nabla\cdot T + \int_{\partial B} dx_B \kappa \mathbf{n}\sigma\delta(x - x_B), \tag{5}$$

where σ represents the interfacial tension between polymer solution and residual oil, ∂B the residual oil surface including point x_B, κ the curvature of residual oil surface, $\boldsymbol{n}$ the outer normal unit vector of residual oil surface, and $\delta(x - x_B)$ is the δ function of the second order. Here, interfacial tension is treated as a mass force for numerical computation and a source item in the motion equation. T represents stress tensor. Since the residual oil film deforms as it flows with polymer solution, transient computation is needed here. The interface between polymer solution and residual oil is coupled with a flow equation, and integral solution of a motion equation should be performed in two steps. In step one, pressure is ignored and velocity field is predicted as [28]

$$\frac{\rho^{n+1}u^* - \rho^n u^n}{\Delta t} = \left\{ \begin{array}{l} -\nabla(\rho uu)^n + \nabla\cdot\tau^n \\ +\left(\int_{\partial B} dx_B \kappa \mathbf{n}\sigma\delta(x - x_B)\right)^n \end{array} \right\}, \tag{6}$$

where Δt represents time step and u^* represents new velocity. Calculate u^n till a new interface is obtained, and obtain $\rho^{n+1}(x)$ via density equation (7) as follows:

$$\rho(x) = \rho_p + \left(\rho_o - \rho_p\right) I(x). \tag{7}$$

In step two, calculate the velocity field via the central difference and obtain

$$\frac{u^{n+1} - u^*}{\Delta t} = -\frac{1}{\rho^{n+1}}\nabla p^{n+1}. \tag{8}$$

Discretize the above equation. With incompressibility

$$\nabla\cdot u^{n+1} = 0, \tag{9}$$

obtain a Poisson equation against pressure

$$\nabla\cdot\left(\frac{1}{\rho^{n+1}}\nabla p^{n+1}\right) = -\frac{1}{\Delta t}(\nabla\cdot u^*). \tag{10}$$

The flow field, including velocity field and stress field, can be calculated via the above flow equation, and then deviatoric stress and horizontal differential stress on the oil film and residual oil deformation can be calculated. Residual oil deformation because of viscoelastic polymer flooding is a nonconstant issue involving fluid-to-fluid interface deformation and reconstructing and complex rheological properties of polymer solution. Therefore, both interfacial tension and time variance should be considered in the flow equation. Computational analysis of the polymer flow field can be made with the flow equation improved according to a real case.

3. Result Analysis

3.1. Flow Field Distribution. The polymer flow field includes velocity field, pressure field, and deviatoric stress field and stream function distribution shown in Figure 2 in which all units are international standard units.

Figure 2 shows that flow channel becomes increasingly narrower in the upstream of the oil film and flooding solution flows at a greater velocity which hits the maximum on the top of the oil film. At the oil film, pressure drop reaches the maximum, with bigger stress T_{11} and smaller T_{22}, and there is rotation in the flowing process. There is parallel linear flow at the entry of flow channel. The flow line gets curved when it is closer to the oil film with the largest curve on the top of the oil film and then folds and returns to parallel linear flow. A bigger velocity difference at the oil film leads to bigger microscale stress on the oil film. A bigger differential pressure leads to bigger macroscopical stress on the oil film. Stress T_{11} is close to differential pressure in terms of the order of magnitude; T_{12} and T_{22} are relatively small. Therefore, T_{11} plays a leading role in the stress and deformation of residual oil.

3.2. The Impact of the Viscosity Ratio on Residual Oil Deformation. The following are the basic parameters: fluid channel is 20 μm wide and 100 μm long, and residual oil film is 40 μm long and 10 μm wide. Computation conditions are as follows: the density of polymer solution is 1100 kg/m^3, and that of residual oil film is 850 kg/m^3. Interfacial tension is 0.001 mN/m, initial wetting angle is 47°, quantity of flow is $2e-10$ m^3/s, viscosity ratio is 0.25, Ca is 1.2, Re is $2.5e-6$, and We is 0.4. Figure 3 shows residual oil deformation at different times.

Figure 3 shows greater residual oil deformation along the viscoelastic polymer flooding direction. Figure 4 shows residual oil deformation when residual oil viscosity remains unchanged, flooding polymer viscosity changes, and thus viscosity ratio changes. Time t is equal to 0.4 s.

It is shown in Figure 4 that Reynolds number (Re) decreases, capillary number (Ca) increases, flooding force increases, and residual oil deforms more obviously as flooding solution viscosity increases and thus viscosity ratio decreases. The advancing angle and receding angle of residual oil are calculated in order to better reflect the deformation scale [29–31]. Measurement of contact angle depends on whether the solid surface is "nonwettable" or "wettable."

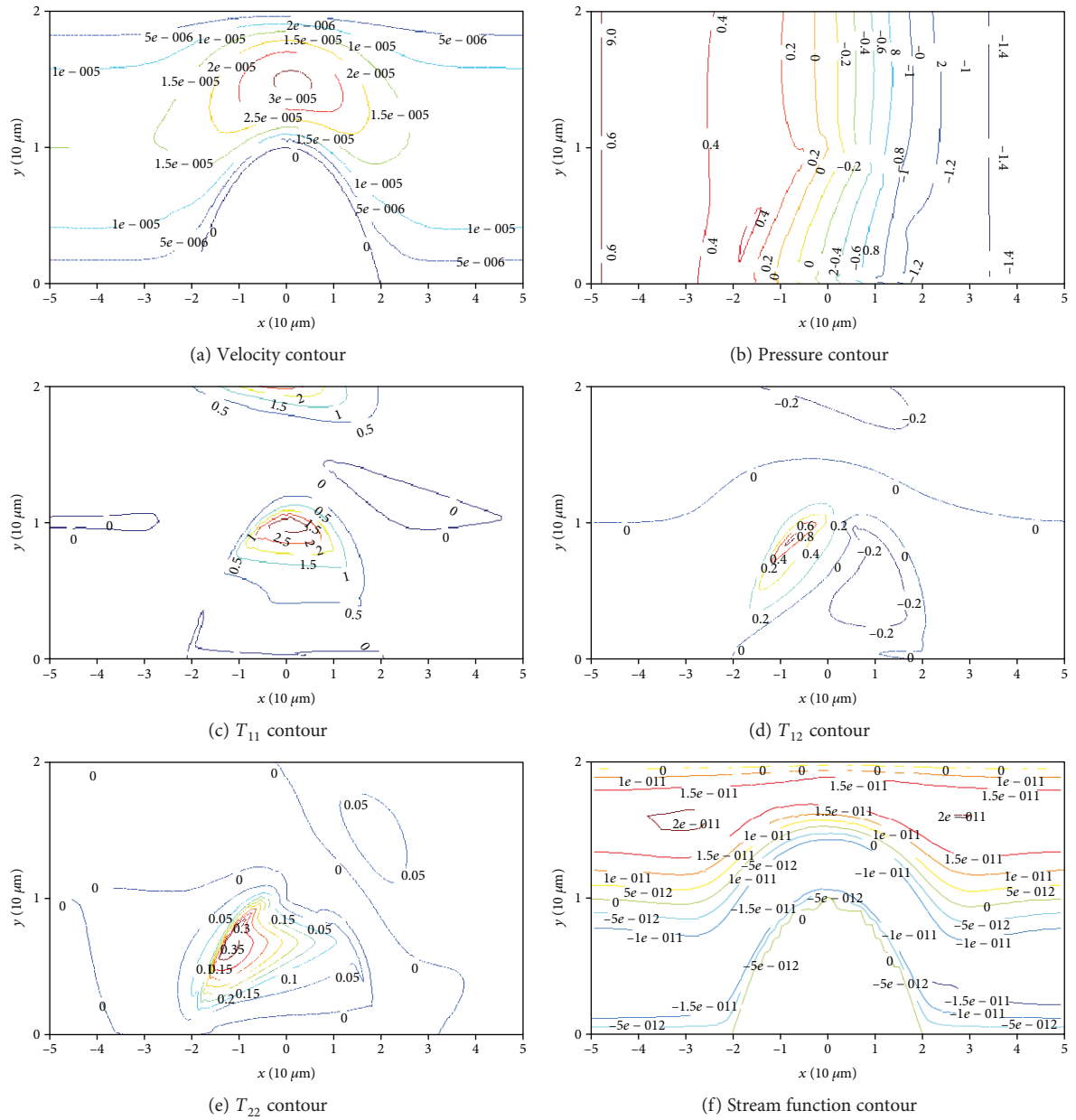

Figure 2: The flow field distribution.

The former is called advancing angle θ_a, and the latter receding angle θ_r, which are shown in Figure 5.

In the former case, the fluid drop becomes bigger if more fluid is injected into it and the contact angle here is called advancing angle represented by θ_a, while in the latter case the fluid drop becomes smaller if fluid is taken out by an injector and the contact angle here is called receding angle represented by θ_r. The advancing angle is not equal to and often larger than the receding angle, which is called contact angle hysteresis. Table 1 shows how contact angle changes with the viscosity ratio.

Table 1 shows that residual oil deformation is increasingly obvious with an increasingly bigger advancing angle and an increasingly smaller receding angle as the viscosity ratio decreases. It is assumed here that three-phase junction is fixed and the interfacial tension between residual oil and rock is large enough. If this interfacial tension is not enough to resist the flooding force of viscoelastic polymer solution, point A will move forward when receding angle decreases to the critical value; point B will move forward when the advancing angle increases to the critical value. In this way, residual oil moves forward and the flooding effect is achieved.

3.3. The Impact of Initial Wettability of Residual Oil Film on Residual Oil Deformation. The following are the basic parameters: fluid channel is 20 μm wide and 100 μm long, and residual oil film is 40 μm long and 10 μm wide. Computation conditions are as follows: the density of polymer solution is

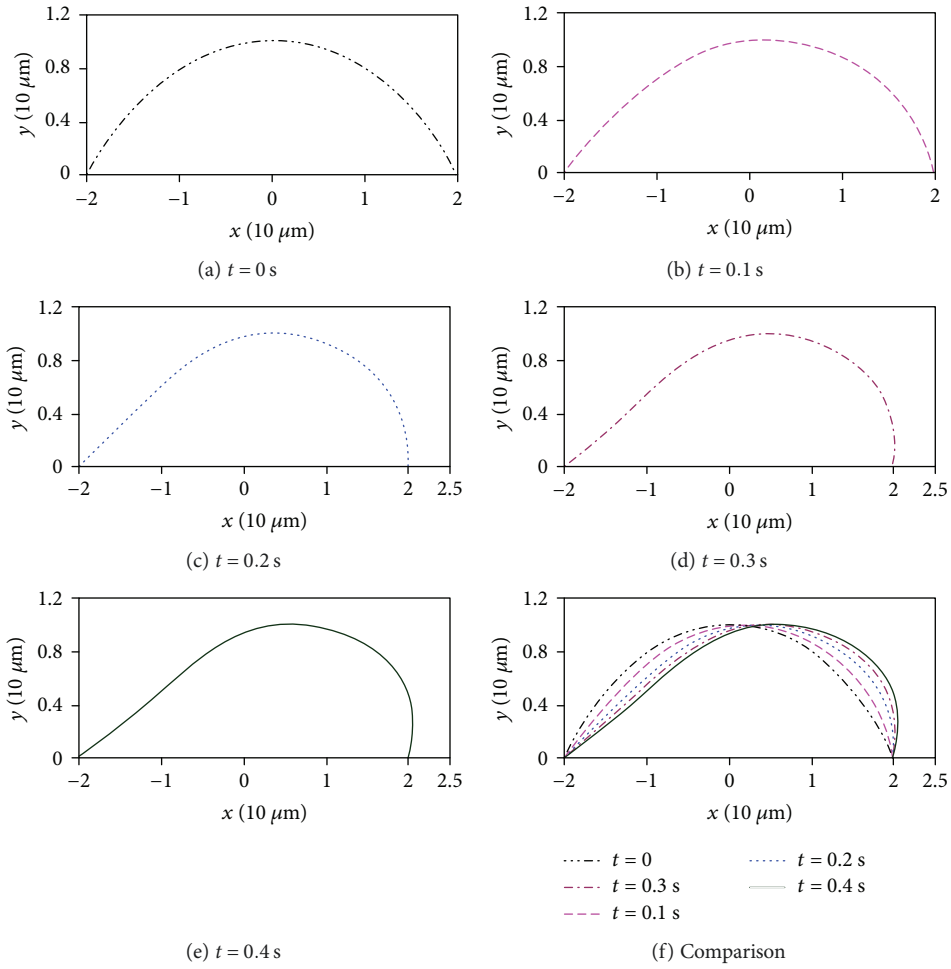

Figure 3: The deformation of residual oil with time.

1100 kg/m^3, and that of residual oil film is 850 kg/m^3. Interfacial tension is 0.001 mN/m, quantity of flow Q is $2e-10$ m^3/s, viscosity ratio is 0.5, We is 0.4, Re is $5e-6$, Ca is 0.6, and t is 0.4 s. For oil films with the same length 40 μm, the wetting angle is set at 30°, 45°, and 60° since initial wettability differs.

Figure 6 shows that bigger initial wetting angle corresponds to bigger residual oil film and more obvious deformation. However, it is biased to observe deformation scale only from the above figures since their initial wetting angles differ. Below are the computed changes of advancing and receding contact angles (Tables 2 and 3).

It is found in Tables 2 and 3 that the bigger initial wetting angle leads to bigger advancing contact angle and smaller receding contact angle. However, when the initial wetting angle is 30°, the advancing angle change reaches the maximum 74.33°; when the initial wetting angle is 60°, the receding angle change reaches the maximum 32.94°. In other words, for oil films with the same length, a smaller initial wetting angle corresponds to the bigger change of the advancing contact angle and more obvious downstream deformation; a bigger initial wetting angle corresponds to a bigger change of the receding contact angle and more obvious upstream deformation. For residual oil on the surface of the oil-wet rock with bigger interfacial tension between residual oil and rock, overall separation is very difficult but local separation is relatively easy. Therefore, a bigger initial wetting angle leads to easier partial separation.

3.4. Calculation of Normal Deviatoric Stress. The variation of normal deviatoric stress under different conditions is shown in Figure 7.

The normal deviatoric stress is the force perpendicular to the surface of residual oil, and it causes the normal convex and concave of residual oil, which benefits local deformation and enlargement of regional oil. Figure 7 shows that the smaller ratio of viscosity of residual oil and polymer solution and the higher polymer solution viscosity result in higher normal deviatoric stress on the residual oil film. Different wetting angles (30°, 45°, and 60°) of the oil film with the same length (40 μm) result in corresponding variations of oil film height, and the higher wetting angle and height of oil film correspond to larger normal deviatoric stress on the oil film. The normal deviatoric stress shows a similar trend in the above conditions. In the upstream of the oil film, the normal deviatoric stress gradually increases to reach the extremum and then decreases, and the oil film is compressed. Around the middle of the oil film, the normal deviatoric stress is negative, and the oil film is in tension. In the downstream

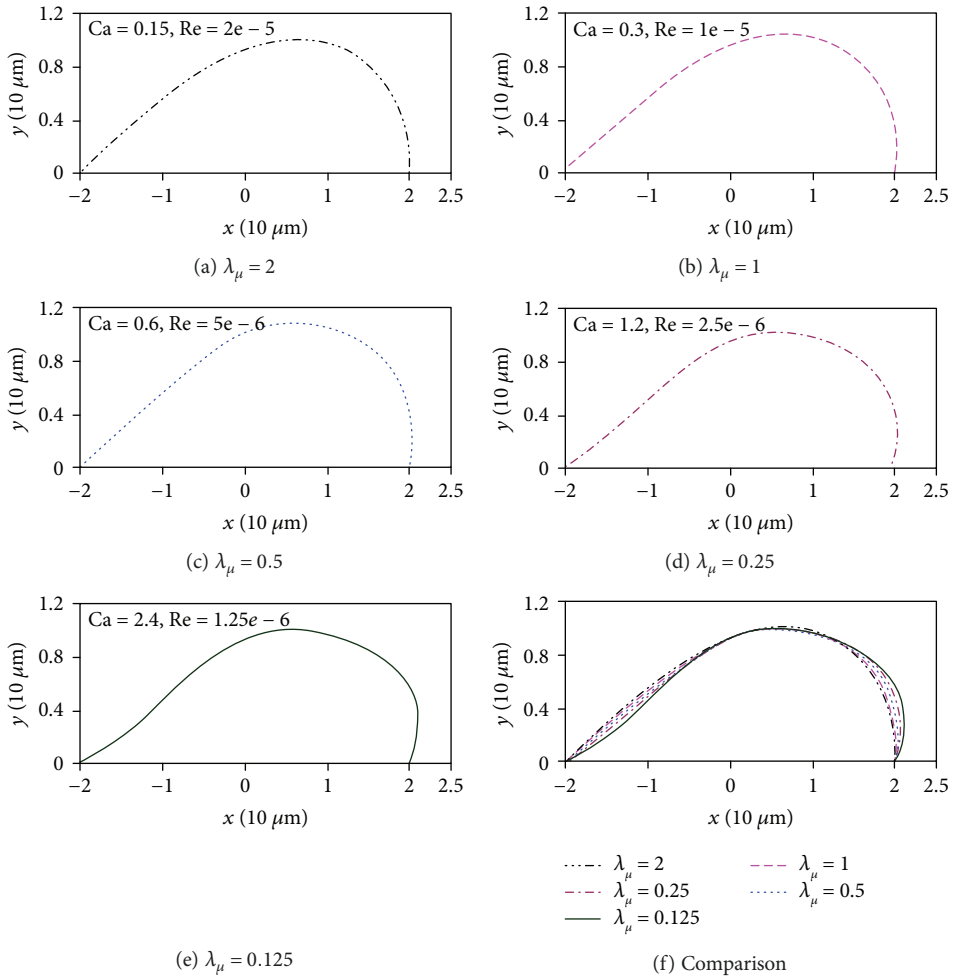

Figure 4: The deformation curve of residual oil with viscosity ratio.

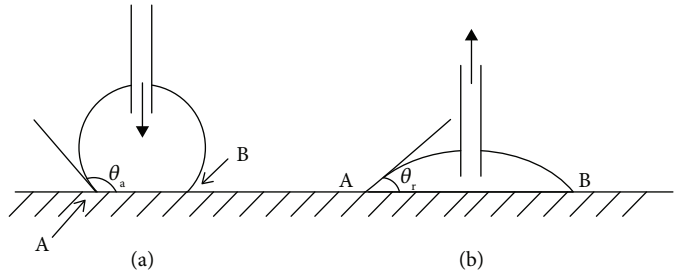

Figure 5: The advancing angle and receding angle.

Table 1: Advancing and receding contact angle (viscosity ratio).

Wetting angle	Viscosity ratio (λ_μ)				
	2	1	0.5	0.25	0.125
Advancing angle θ_a (°)	93.68	99.25	106.70	113.08	121.29
Receding angle θ_r (°)	31.77	28.77	25.58	22.51	18.95

of the oil film, the normal deviatoric stress is positive, and the oil film is compressed. This causes compression in both ends and tension in the middle. The distribution of normal deviatoric stress benefits the convex of the oil film in the middle, and the oil film is deformed by flooding fluid and separates from the main body.

3.5. Calculation of Tangential Deviatoric Stress. The variation of tangential deviatoric stress under different conditions is shown in Figure 8.

The tangential deviatoric stress is the force along the tangent line of the residual oil film, and the higher tangential deviatoric stress results in a larger angular deformation. The trend of tangential deviatoric stress in Figure 8 shows

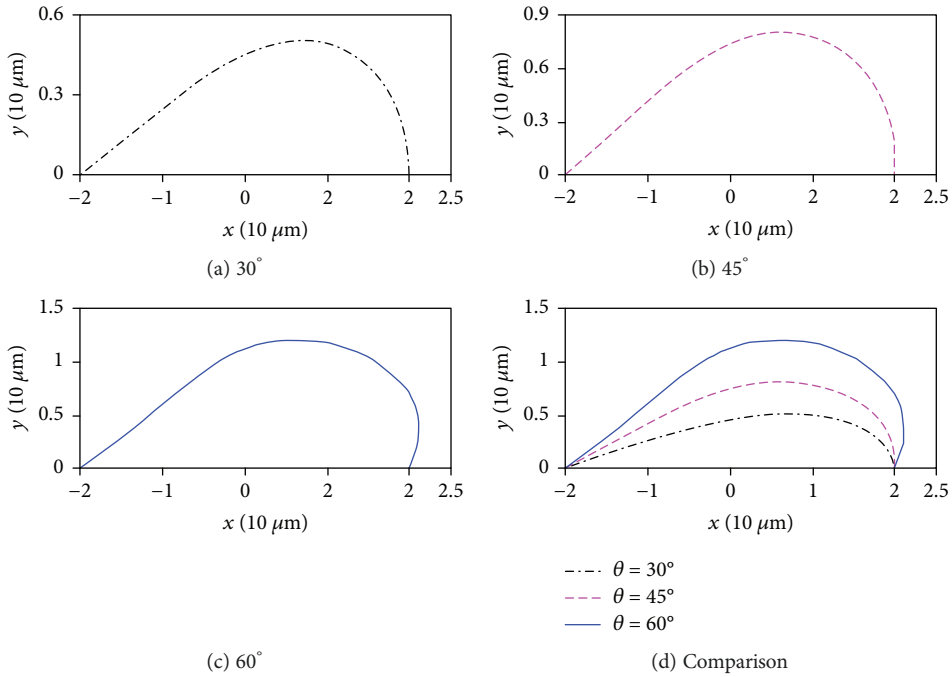

Figure 6: The deformation curve of residual oil with initial wetting angle.

Table 2: Advancing and receding contact angle (initial wetting angle).

Wetting angle	Initial wetting angle θ (°)		
	30	45	60
Advancing angle θ_a (°)	104.33	110.57	127.98
Receding angle θ_r (°)	15.36	20.42	27.06

Table 3: The change of advancing and receding contact angle (initial wetting angle).

Wetting angle	Initial wetting angle θ (°)		
	30	45	60
Advancing angle change θ_a (°)	74.33	64.43	67.98
Receding angle change θ_r (°)	14.64	13.58	32.94

that there is a dividing point between 1/4 and 1/2 lengths along the flowing direction, and the tangential deviatoric stress is negative before the point and positive behind the point. The smaller ratio of viscosity of residual oil and polymer solution and the stronger elasticity result in higher tangential deviatoric stress on the residual oil film. Due to the memory function of viscoelastic fluid, the elasticity of flooding fluid has a hysteretic influence on the peak of tangential deviatoric stress. The larger wetting angle of the oil film with the same length (40 μm) results in larger tangential deviatoric stress on the oil film.

3.6. Calculation of Horizontal Deviatoric Stress. The variation of horizontal deviatoric stress under different conditions is shown in Figure 9.

Figure 9 shows the positive value of horizontal deviatoric stress except for the part near the rock, indicating that the horizontal component of the force of polymer solution on the residual oil is in the same direction as the flowing. The negative value in the part near the rock is due to the interfacial tension in the triphase contact area. The horizontal deviatoric stress is axisymmetrically distributed along the middle of the oil film with the maximum value. The horizontal deviatoric stress variation has the similar trend as the normal deviatoric stress does.

3.7. Calculation of Vertical Deviatoric Stress. The variation of vertical deviatoric stress under different conditions is shown in Figure 10.

Figure 10 shows that the vertical deviatoric stress variation is positive in a small part of the middle of the oil film and negative in the rest part, suggesting that the vertical component of force of polymer solution on the residual oil has a downward direction. The absolute value of vertical deviatoric stress in the upstream of the oil film is higher than that in the downstream of the oil film, indicating higher pressure. The comparison with horizontal deviatoric stress shows that the absolute value of vertical deviatoric stress is higher than that of horizontal deviatoric stress in the same position. The normal and tangential components of both horizontal and vertical deviatoric stresses have the same direction as both normal and tangential deviatoric stresses.

The oil has the smallest interfacial energy with a static residual oil film and polymer solution in the equilibrium state. The superficial area of the residual oil film tends to decrease as much as possible and a shrinkage force along the tangential direction, that is, interfacial force stops the deformation of the interface. The shape of the contact area

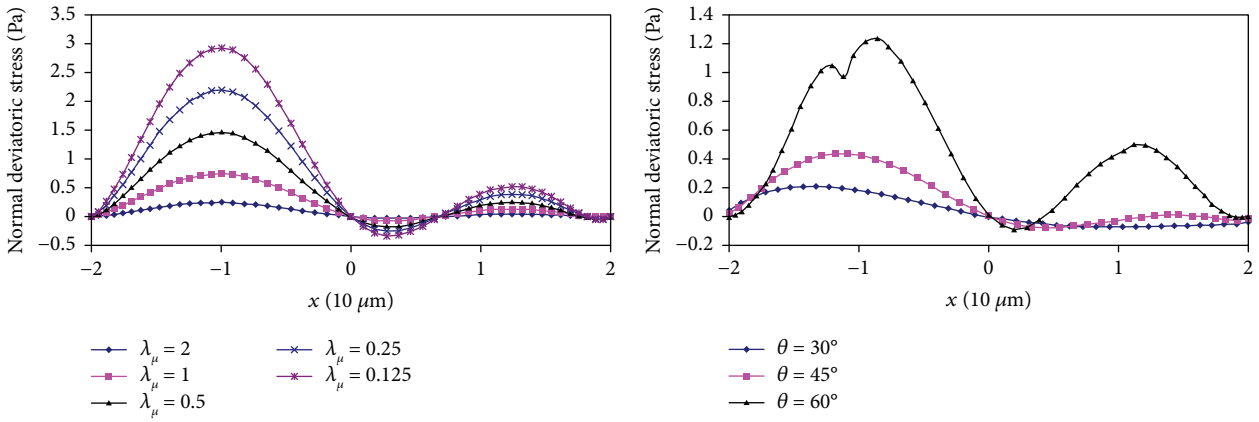

(a) Variation of viscosity ratio

(b) Variation of initial wetting angle

Figure 7: Curves of normal deviatoric stress variation.

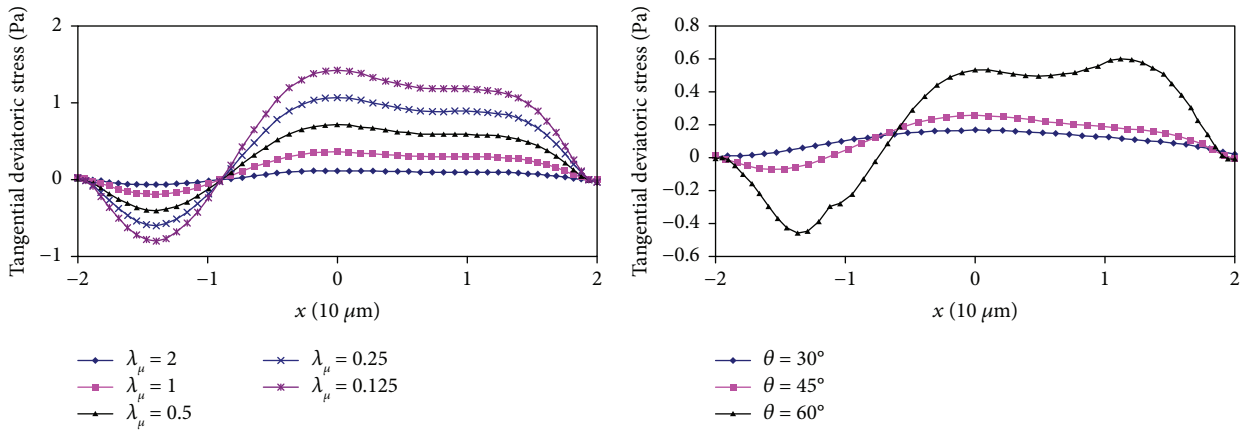

(a) Variation of viscosity ratio

(b) Variation of initial wetting angle

Figure 8: Curves of tangential deviatoric stress variation.

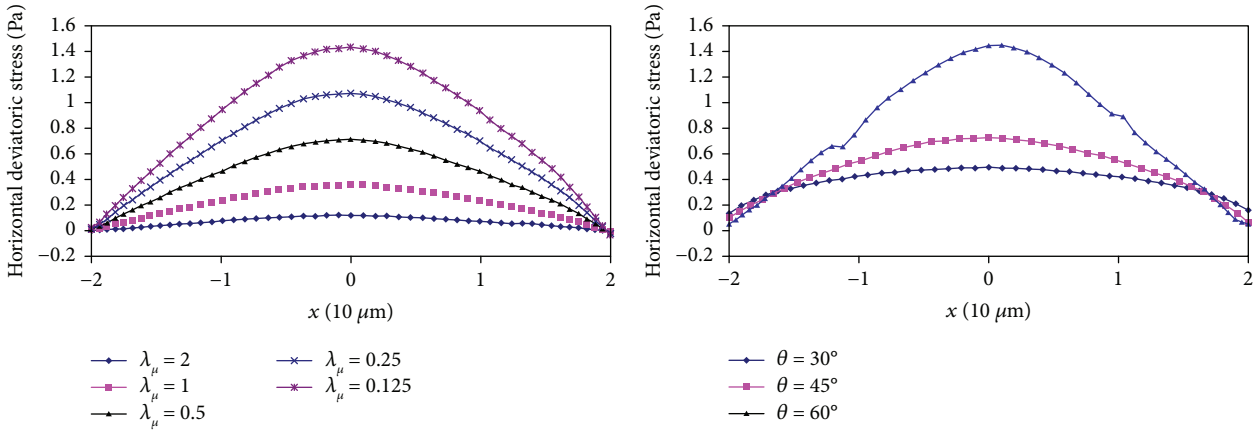

(a) Variation of viscosity ratio

(b) Variation of wetting angle

Figure 9: Curves of horizontal deviatoric stress variation.

of the rock, oil, and flooding fluid results from the balance between the interaction force (adhesive force) of oil molecules in the adhesive layer and the rock molecules and the mutual attraction (cohesion force) of oil molecules. If the adhesive force is higher than the cohesion force, the rock is wetted by the oil with the expanded adhesive layer.

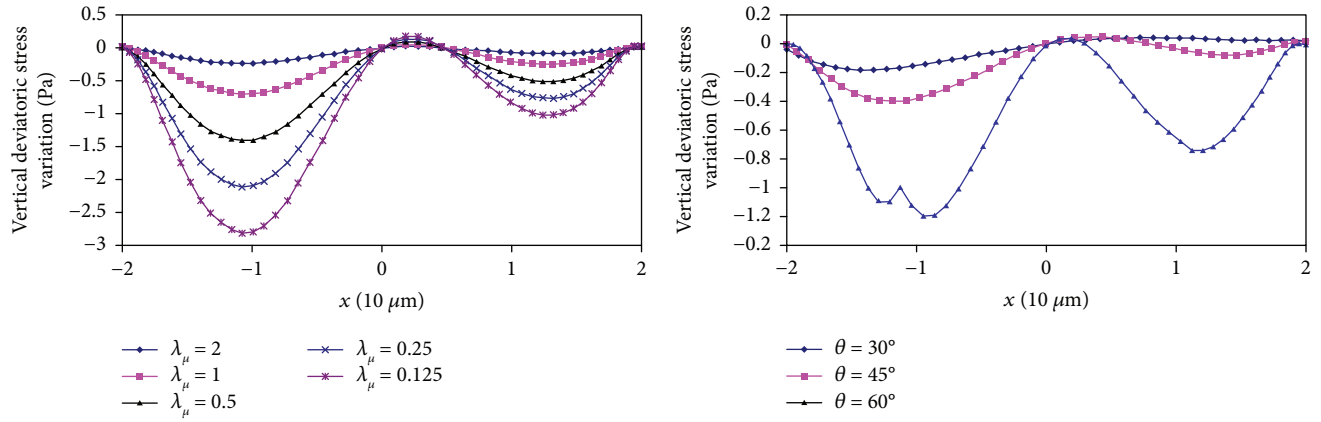

(a) Variation of viscosity ratio

(b) Variation of wetting angle

Figure 10: Curves of vertical deviatoric stress variation.

Conversely, the adhesive force is lower than the cohesion force, and the rock is not wetted by the oil with the shrunk adhesive layer. When the flooding fluid sweeps through the residual oil, both shear and tension forces are generated, changing the shape of residual oil, and the wetting angle is changed correspondingly, causing wettability hysteresis. The wettability hysteresis is not obvious with higher interfacial tension, while wettability hysteresis is obvious with lower interfacial tension when the residual oil is possibly completely separated. There is a critical capillary number for the deformation and separation of residual oil. With the capillary number below the critical value, the residual oil is further stretched and reaches the steady state. Otherwise, the residual oil continues to be stretched. For a long time, the latter part of residual oil is pushed downstream, and a negative curvature is generated toward the rock wall face. The front part of residual oil rolls along the rock wall face. With the high interfacial tension between the rock and residual oil, the residual oil is broken, and a part is separated from the parent fluid drop, and another part is still adhered to the rock wall.

4. Conclusions

With the same quantity of flow, this paper analyzes the impact of the viscosity of flooding solution and the wettability of residual oil on the stress of residual oil. The computation shows that residual oil deformation is increasingly more obvious with an increasingly bigger advancing angle and an increasingly smaller receding angle as the viscosity ratio decreases. Through the analysis of the impact of the initial wetting angle on residual oil deformation, it is concluded that the bigger initial wetting angle corresponds to the bigger advancing angle and smaller receding angle. For oil films with the same length, the smaller initial wetting angle corresponds to the bigger change of the advancing contact angle and more obvious downstream deformation; the bigger initial wetting angle corresponds to the bigger change of the receding contact angle and more obvious upstream deformation. Such analysis offers certain guidance to the preparation of polymer solution and understanding of residual oil film distribution in microchannels and increases flooding efficiency and oil recovery.

The horizontal stress difference reflects the force on the flooded residual oil of different heights toward the flowing direction. The horizontal stress difference increases with the flooding fluid viscosity. As the viscosity increases by one time, the horizontal stress difference increases by one time correspondingly. The increase of flooding fluid elasticity results in the change of the horizontal stress difference, which increases to the extremum and then decreases gradually. The point of the extremum is not located at the triphase contact point, but somewhere in the upstream of the residual oil film, which is related with the memory function of viscoelastic fluid. The higher elasticity of flooding fluid results in a larger extremum of horizontal stress difference.

Conflicts of Interest

The authors declare that they have no competing interests.

Acknowledgments

This work was supported by University Nursing Program for Young Scholars with Creative Talents in Heilongjiang Province through Grant no. UNPYSCT2016121.

References

[1] L. J. Zhang and X. A. Yue, "Displacement of polymer solution on residual oil trapped in dead ends," *Journal of Central South University*, vol. 15, Supplement 1, pp. 84–87, 2008.

[2] B. Y. Jamaloei and R. Kharrat, "Analysis of microscopic displacement mechanisms of dilute surfactant flooding in oil-wet and water-wet porous media," *Transport in Porous Media*, vol. 81, no. 1, pp. 1–19, 2010.

[3] S. M. Shi, H. B. Wei, B. Li, H. Lou, and D. K. Huo, "Research on residual oil distribution regular of steam flooding after polymer flooding," *Advanced Materials Research*, vol. 734-737, pp. 1440–1444, 2013.

[4] P. Seppecher, "Moving contact lines in the Cahn-Hilliard theory," *International Journal of Engineering Science*, vol. 34, no. 9, pp. 977–992, 1996.

[5] T. H. Chou, S. J. Hong, Y. J. Sheng, and H. K. Tsao, "Drops sitting on a tilted plate: receding and advancing pinning," *Langmuir*, vol. 28, no. 11, pp. 5158–5166, 2012.

[6] D. J. E. Harvie, M. R. Davidson, J. J. Cooper-White, and M. Rudman, "A parametric study of droplet deformation through a microfluidic contraction: shear thinning liquids," *International Journal of Multiphase Flow*, vol. 33, no. 5, pp. 545–556, 2007.

[7] P. Garstecki, M. J. Fuerstman, H. A. Stone, and G. M. Whitesides, "Formation of droplets and bubbles in a microfluidic T-junction-scaling and mechanism of break-up," *Lab on a Chip*, vol. 6, no. 3, pp. 437–446, 2006.

[8] C. Fang, C. Hidrovo, F.-m. Wang, J. Eaton, and K. Goodson, "3-D numerical simulation of contact angle hysteresis for microscale two phase flow," *International Journal of Multiphase Flow*, vol. 34, no. 7, pp. 690–705, 2008.

[9] G. K. Seevaratnam, H. Ding, O. Michel, J. Y. Y. Heng, and O. K. Matar, "Laminar flow deformation of a droplet adhering to a wall in a channel," *Chemical Engineering Science*, vol. 65, no. 16, pp. 4523–4534, 2010.

[10] T. Cubaud, B. M. Jose, S. Darvishi, and R. Sun, "Droplet breakup and viscosity-stratified flows in microchannels," *International Journal of Multiphase Flow*, vol. 39, pp. 29–36, 2012.

[11] D. Wang, J. Cheng, and Q. Yang, "Viscous-elastic polymer can increase microscale displacement efficiency in cores," in *SPE Annual Technical Conference and Exhibition*, pp. 2–8, Dallas, TX, USA, October 2000.

[12] D. Wang, H. Xia, and S. Yang, "The influence of visco-elasticity on micro forces and displacement efficiency in pores, cores and in the field," in *SPE EOR Conference at Oil & Gas West Asia*, pp. 1–18, Muscat, Oman, 2010.

[13] D. Wang, G. Wang, and X. Wu, "Influence of the micro-force produced by viscoelastic displacement liquid on displacement efficiency," *Journal of Xi'an Shiyou University (Natural Science Edition)*, vol. 23, pp. 43–53, 2008.

[14] S. Yang, D. Wang, and H. Xia, "Hydrodynamics mechanism of viscoelastic fluids displacing residual oil droplets in micro pores," *Journal of China University of Petroleum(Edition of Natural Science)*, vol. 35, pp. 139–142, 2011.

[15] L. Liu, S. Yang, and J. Fan, "Stress calculation of polymer displacing residual oil in micro pores," *International Journal of Performability Engineering*, vol. 13, pp. 211–220, 2017.

[16] M. A. Rother, A. Z. Zinchenko, and R. H. Davis, "Surfactant effects on buoyancy-driven viscous interactions of deformable drops," *Colloids and Surfaces A: Physicochemical and Engineering Aspects*, vol. 282-283, pp. 50–60, 2006.

[17] X. Li and K. Sarkar, "Effects of inertia on the rheology of a dilute emulsion of drops in shear," *Journal of Rheology*, vol. 49, no. 6, pp. 1377–1394, 2005.

[18] X. Li and K. Sarkar, "Drop dynamics in an oscillating extensional flow at finite Reynolds numbers," *Physics of Fluids*, vol. 17, no. 2, pp. 027103–027183, 2005.

[19] X. Li and K. Sarkar, "Negative normal stress elasticity of emulsions of viscous drops at finite inertia," *Physical Review Letters*, vol. 95, no. 25, 2005.

[20] T. Fu, Y. Wu, Y. Ma, and H. Z. Li, "Droplet formation and breakup dynamics in microfluidic flow-focusing devices: from dripping to jetting," *Chemical Engineering Science*, vol. 84, pp. 207–217, 2012.

[21] H. Qi and M. Xu, "Stokes' first problem for a viscoelastic fluid with the generalized Oldroyd-B model," *Acta Mechanica Sinica*, vol. 23, no. 5, pp. 463–469, 2007.

[22] M.-K. Zhang, X.-R. Shen, J.-F. Ma, and B.-Z. Zhang, "Flow of Oldroyd-B fluid in rotating curved square ducts," *Journal of Hydrodynamics, Ser. B*, vol. 19, no. 1, pp. 36–41, 2007.

[23] T. Hayat, S. Zaib, S. Asghar, and A. A. Hendi, "Exact solutions in generalized Oldroyd-B fluid," *Applied Mathematics and Mechanics*, vol. 33, no. 4, pp. 411–426, 2012.

[24] J. Hou, "Network modeling of residual oil displacement after polymer flooding," *Journal of Petroleum Science & Engineering*, vol. 59, no. 3-4, pp. 321–332, 2007.

[25] A. K. Gupta and S. Basu, "Deformation of an oil droplet on a solid substrate in simple shear flow," *Chemical Engineering Science*, vol. 63, no. 22, pp. 5496–5502, 2008.

[26] C. Chung, M. Lee, K. Char, K. H. Ahn, and S. J. Lee, "Droplet dynamics passing through obstructions in confined microchannel flow," *Microfluidics and Nanofluidics*, vol. 9, no. 6, pp. 1151–1163, 2010.

[27] A. E. Komrakova, O. Shardt, D. Eskin, and J. J. Derksen, "Effects of dispersed phase viscosity on drop deformation and breakup in inertial shear flow," *Chemical Engineering Science*, vol. 126, pp. 150–159, 2015.

[28] J. Fan, Y. Liu, L. Liu, and S. Yang, "Hydrodynamics of residual oil droplet displaced by polymer solution in micro-channels of lipophilic rocks," *International Journal of Heat and Technology*, vol. 35, no. 3, pp. 611–618, 2017.

[29] D. Quéré, M.-J. Azzopardi, and L. Delattre, "Drops at rest on a tilted plane," *Langmuir*, vol. 14, no. 8, pp. 2213–2216, 1998.

[30] P. A. Durbin, "Free-streamline analysis of deformation and dislodging by wind force of drops on a surface," *Physics of Fluids*, vol. 31, no. 1, pp. 43–48, 1988.

[31] P. A. Durbin, "On the wind force needed to dislodge a drop adhered to a surface," *Journal of Fluid Mechanics*, vol. 196, no. 1, pp. 205–222, 1988.